PERGAMON

Journal of Structural Geology 23 (2001) 845–856

JOURNAL OF STRUCTURAL GEOLOGY

www.elsevier.nl/locate/jstrugeo

The role of initial perturbations in the development of folds in a rock-analogue

P.F. Williams[a,*], D. Jiang[b]

[a]*Department of Geology, The University of New Brunswick, Fredericton, New Brunswick, Canada E3B 5A3*
[b]*Department of Geology, University of Maryland, College Park, MD 20742, USA*

Received 22 January 1999; accepted 21 September 2000

Abstract

A series of experiments is described in which layered specimens were shortened parallel to the layering. The specimens comprise two salt (NaCl) layers sandwiched between three layers of salt–mica synthetic schist. All specimens were prepared and deformed under the same conditions, except for the amount of shortening, which was varied. The resulting fold-shapes are variable, even where the amounts of shortening are the same. In one specimen, folds are believed to have developed essentially by buckling with very little concomitant bulk homogeneous shortening perpendicular to the axial-plane. The specimen lacks an axial-plane foliation. Other folds are believed to have experienced varying amounts of bulk homogeneous shortening before and during buckling, and all have axial-plane foliations that have developed by grain-scale transposition of the original bedding-parallel mica foliation. The difference in the behaviour of the various specimens is explained in terms of initial perturbations. These irregularities take the form of initial deflections in the almost planar bedding, variation in the degree of preferred orientation of the mica grains, and local compositional variation within individual salt–mica layers.

1. Introduction

Much of the research on folding and most modelling of folds has been concerned with planar, parallel-sided layers or multilayer systems. Physical and numerical modelling of such systems has led to the considerable understanding of the relationships between fold-shape, deformation path and variation in the rheology of the different layers and is dealt with in various textbooks (e.g. Johnson, 1970; Ramsay and Huber, 1987; Twiss and Moores, 1992; Ghosh, 1993). The rheology is most commonly modelled in terms of Newtonian fluids (e.g. Biot, 1957, 1961; Ramberg, 1959, 1963, 1964; Biot et al., 1961; Sherwin and Chapple, 1968; Hudleston, 1973; Hudleston and Stephansson, 1973; Treagus, 1981, 1997; Cobbold, 1983), but other more complex rheologies have also been considered (e.g. Chapple, 1969; Parrish, 1973; Fletcher, 1974; Smith, 1977, 1979; Treagus and Sokoutis, 1992; Treagus, 1993; Hudleston and Lan, 1994). Fold-shape and wavelength/thickness ratio are commonly believed to be determined by the relative rheologies of the layers involved, and the models generally ignore any irregularities in the layers. However, Abbassi and Mancktelow (1990) and Mancktelow (1999) considered the role of large perturbations in the folding of a single layer, embedded in a matrix of lower viscosity. Cobbold et al. (1971) and Cobbold (1976) considered the role of anisotropy in the development of folds and experimentally deformed statistically homogeneous (Turner and Weiss, 1963, pp. 16–17) anisotropic specimens made up of viscous materials. In this paper, we describe a series of physical experiments, on a crystalline rock-analogue, that has essentially isotropic layers (salt) sandwiched in a statistically anisotropic matrix (salt–mica mix). We interpret the results as an indication that irregularities in geometry and rheology can be important in determining the morphology of folds in nature and may give rise to folds that do not reflect the wavelength/thickness relationship, commonly considered applicable to natural situations.

The project described here was initially designed to examine fold and microstructural development as a function of increasing strain, by performing a series of physical experiments that were identical in everything but strain magnitude. To be successful, the experiments had to be reproducible since the assumption was that a low-strain experiment represented an initial stage of a high-strain experiment. The experiments, in fact, were not reproducible and an investigation into the cause of the non-reproducibility led to the ideas presented here.

* Corresponding author. Fax: +1-506-453-5055.
E-mail address: pfw@unb.ca (P.F. Williams).

0191-8141/01/$ - see front matter
PII: S0191-8141(00)00157-7

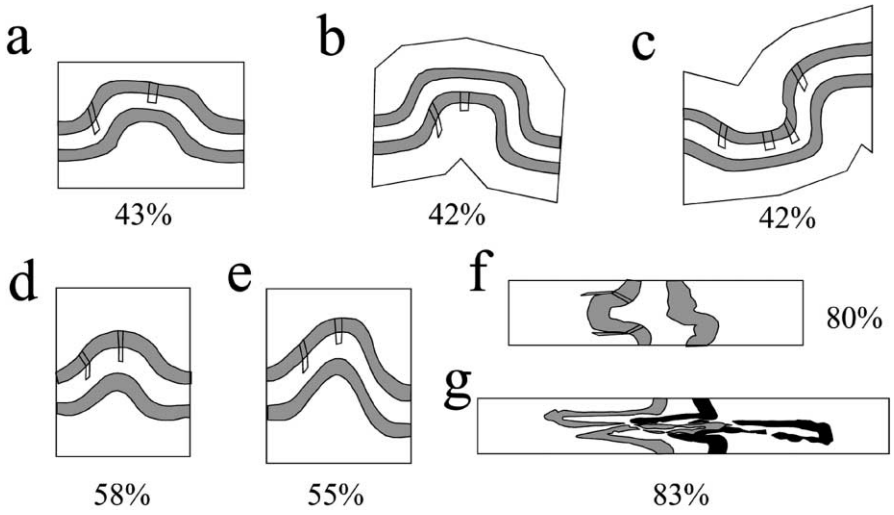

Fig. 1. Deformed specimens. Shaded areas represent salt layers; two shades are used in (g) to facilitate separation of layers. The specimen outlines are approximate since they are partially destroyed in extracting the specimens and preparing thin-sections. Numbers below or adjacent to each figure are the amounts of shortening. The small quadrilaterals in figures a–f join markers that, in the undeformed specimen, defined rectangles, orthogonal with layering. Deformation in figure g is too heterogeneous to recognise the quadrilaterals with confidence. Diagrams f and g represent specimens 248 and 253, respectively, which are referred to by number in the text.

The materials used were salt (NaCl) and mica rock-analogues deformed in a large capacity gas-deformation-rig. We start by describing the experimental procedure and resulting folds and microstructures. We then consider the causes of folding in the experimental materials, and finally the possible significance of our conclusions for folding in rocks.

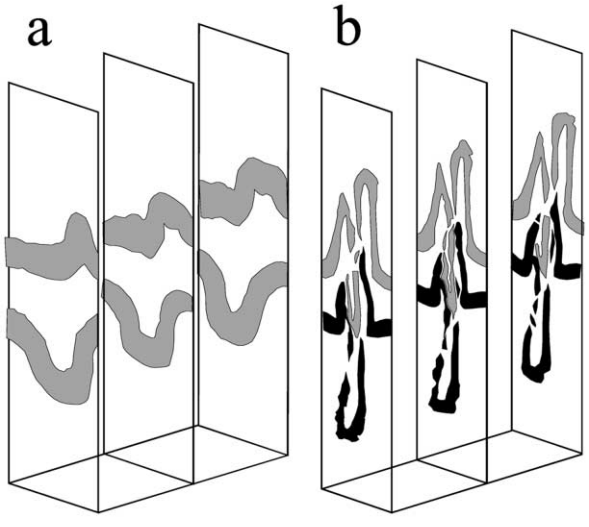

Fig. 2. Two end views and a medial section, stacked in a 3D array, for specimens (a) 248 and (b) 253. Shaded areas represent salt layers; two shades are used in (b) to facilitate separation of layers. Note the spacing between the sections is exaggerated by a factor of approximately two. See text for further discussion.

2. Experimental procedure

The specimens comprise five compositional layers made by stacking 12 wafers of which numbers 5 and 8 are salt and the remaining 10 are a mixture of salt and mica. The salt was ground to a maximum grain size of approximately 100 μm. The mica is a synthetic fluorine phlogopite with larger flakes approximately 500 μm in their longest dimension. The salt–mica mix is the same one described more elaborately by Means and Williams (1972) and Williams et al. (1977). It is composed of approximately 57% (by volume) salt and the rest is mica.

The wafers were made individually of salt and salt–mica mix by compacting the materials, in powder form, in a rectangular pellet-press at a pressure (friction neglected) of 360 MPa. The resulting wafers typically measured ca. $7.8 \times 1.9 \times 0.2$ cm with the last dimension being variable (0.18–0.27 cm) since it was determined by the amount of powder and the evenness of the distribution of the powder in the pellet-press. The thickness of individual wafers was measured at both ends and in the middle and found to vary by up to 560 μm. Typically, however, it varied by less than 100 μm. Fabrication of the salt–mica wafers resulted in a strong preferred orientation of the mica flakes with (0 0 1) perpendicular to the short dimension of the wafer. Lines were stamped on the large surfaces of the individual wafers, perpendicular to the long dimension; red lines on one side, green on the other. Line spacing was 0.1 in. (ca. 0.25 cm), and the ends of the lines, visible as dots on the long surfaces of the specimens perpendicular to layering, define a rectangular grid.

The wafers were stacked, with all faces with red lines on one side, and all faces with green lines on the other side, so

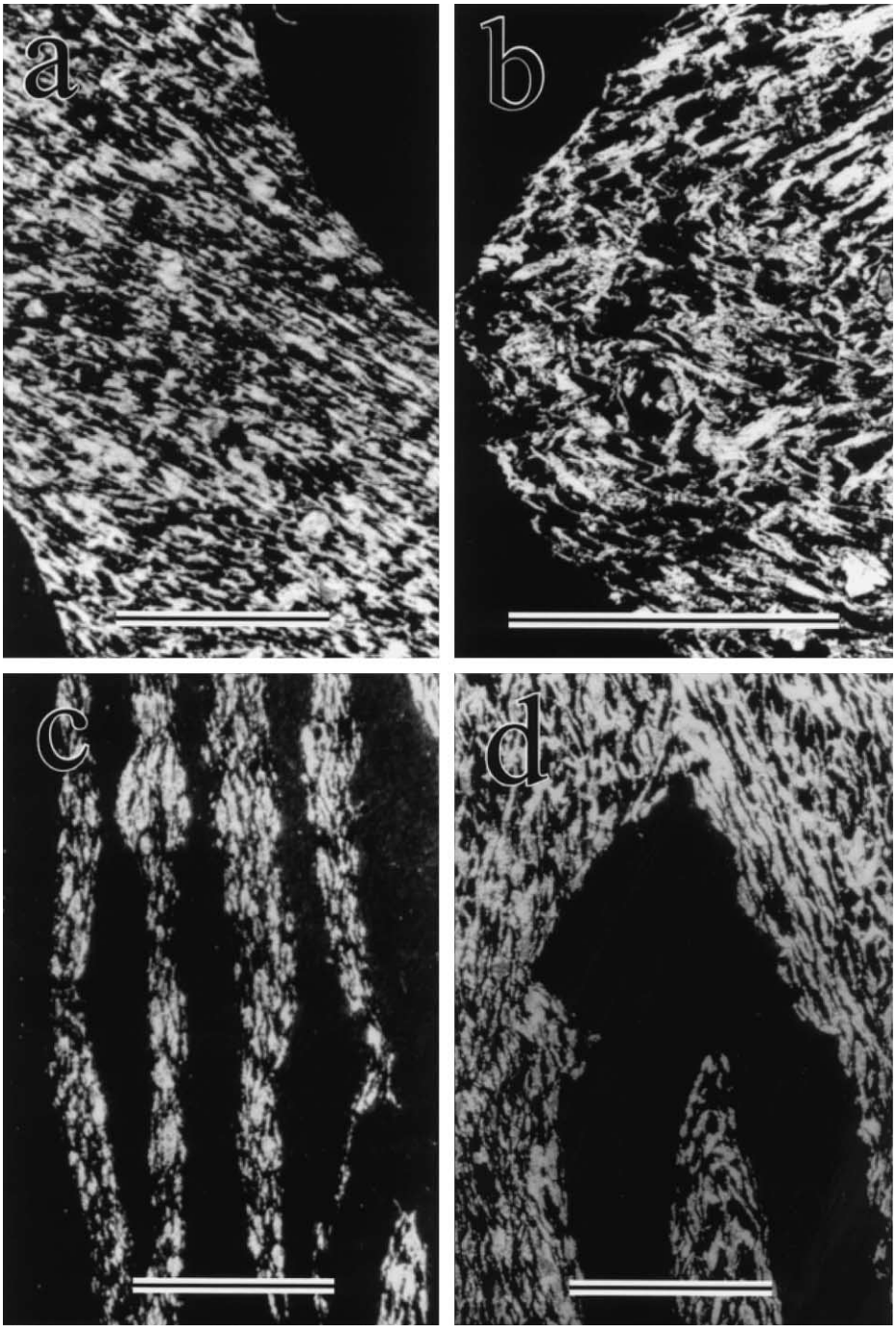

Fig. 3. Microphotographs (crossed polars) of the mica fabric in the salt–mica layers. Black areas are salt. (a) Specimen 248 showing a well-developed foliation in the salt–mica layer between the two salt layers on a fold limb. The axial-planes of the two folds are oblique to the photograph and parallel to the mica foliation which slopes down to the right. (b) A fold hinge in specimen 248, showing the bimodal mica fabric, due to parasitic kinking, symmetrical about the axial plane of the fold. (c) Boudinaged fold limbs in specimen 253 with the mica fabric parallel to the transposed layering. (d) Fold hinge in specimen 253 with the mica fabric wrapping around the fold and forming a single kink in the fold hinge. Scale bars are 3 mm long in (a) and (b) and 2.5 mm in (c) and (d).

that on each contact ("bedding plane") there were coincident red and green lines (non-coincidence of the lines after deformation made it possible to recognise where there had been slip on these surfaces during the experiment). The assembled specimen ($7.8 \times 1.9 \times$ ca. 2.5 cm) was then placed in a precast cylinder of lead with an external diameter of ca. 5 cm and a length of 7.8 cm. Thin pieces of lead sheet were placed over the ends of the assembly, which was then placed between pistons and jacketed with rubber. The assembly is the same as illustrated in Means (1975), except for the lead sheet end pieces, which were inserted in the current series of experiments to reduce friction on the piston faces.

Deformation was carried out dry in the gas-deformation-rig, described by Means (1975), at 103 MPa confining

pressure, room temperature and a strain-rate of $1.2 \times 10^{-4}\ s^{-1}$. Examination of undeformed specimens has shown that the confining pressure is sufficient to weld the constituent wafers into a single block, and specimens that have been subjected to confining pressure only, can be handled during preparation of thin-sections without the danger of separation on bedding planes. Specimens were subjected to layer-parallel shortening by amounts varying between 0 and 83% and were free to expand radially, perpendicular to the direction of shortening.

3. Description of deformed specimens

3.1. Fold-shape

All but the lowest-strain experiments resulted in folding of the layering (Fig. 1), but there is considerable variation in the shape of the folds. They are generally quite cylindrical, and from 10 folded specimens there is only one exception, which is shown in Fig. 2(a). In profile, the folds are neither parallel nor similar, but all layers are commonly thicker in the hinge than on the limbs (Fig. 1). The folds can be divided into inner and outer zones separated by the central bedding plane (which is approximately half-way between the two salt layers), where the inner zone is on the concave side of the dividing surface. In this inner zone, salt and salt–mica layers are generally thicker in the hinges than on the limbs. In the outer zone, the difference is less pronounced in the salt layers (e.g. Fig. 1(e)) and, in the salt–mica layers, layering may be thinner in the hinge than on the limbs on the convex side of the two salt layers.

In profile, folds may be symmetrical, asymmetrical or box-like (Fig. 1) and there is no consistent, simple relationship between fold tightness and the amount of shortening (compare Fig. 1(d)–(g)). The number of folds per specimen varies. Boxfolds such as those shown in Fig. 1(b) have four hinges. Asymmetrical folds (e.g. Fig. 1(c)) have two well-developed hinges and a third and even a fourth hinge in one layer. Most symmetrical folds (e.g. Fig. 1(d) and (e)) have one well-developed fold flanked by two folds that are generally less well, but variably developed. One specimen (Figs. 1(f) and 2(a)) has six folds in one salt/salt–mica contact and seven in the other contact of the same salt layer. One of these folds is large and the others are small and have wavelengths shorter than the thickness of the layer. The other salt layer in the same specimen has only three folds, the central one of which is approximately symmetrical. Another specimen (Fig. 1(g)) has three well-developed, reasonably symmetrical, isoclinal folds flanked on either side by two variably developed more open folds. The flanking folds in all specimens are presumably strongly influenced by proximity to the pistons.

3.2. Strain

Generally, when viewed on the profile plane, the rectangles defined by the ends of marker-lines, show evidence of shortening perpendicular to the axial-planes of the folds and extension parallel to the axial-planes (e.g. Fig. 1(d) and (e)). There are exceptions, however, and in the layers furthest removed from the cores of folds, there may be localised extension perpendicular to the axial-plane. There is some extension parallel to the fold axes; it is heterogeneous and small, the maximum being less than 20% even at 85% shortening. The amount of extension in this direction is the same in both the salt and the salt–mica layers, and there is no tendency for either to extrude. On the limbs of folds, the initial rectangles are generally converted to parallelograms (Fig. 1 (a)–(e)). In the hinges of symmetrical folds they remain rectangles (Fig. 1(d) and (e)), but are generally parallelograms in the hinges of the asymmetrical folds (Fig. 1(c)), possibly indicating hinge migration in these specimens.

Grid lines initially perpendicular to layering are commonly refracted on the fold limbs. Where refracted, the lines are generally more nearly perpendicular to S_0 in the salt layers than in the salt–mica layers. The difference between the two types of layers tends to increase with increasing strain (compare d, e and f in Fig. 1). An offset of continuous lines stamped on the outside of some specimens, and of the red and green lines on the same bedding planes in others, indicate that there is some slip on bedding planes between salt and salt–mica layers, on some fold limbs. The slip, which can be as much as half-a-grid space, is rare and localised, and no pattern has been recognised. For example, it may be present on one limb of a symmetrical fold and not on the other limb. In this situation, the lack of discontinuous slip on the one limb is compensated by increased bedding-parallel penetrative shear in the salt–mica layers on that limb.

3.3. Microstructure

After compaction in the pellet-press, but before deformation, the mica fabric in the salt–mica schist can be described as a bow-tie distribution parallel to bedding, such as is commonly seen in undeformed pelitic sediments. That is, most mica grains are aligned such that their long dimensions (and therefore (0 0 1)) make a small angle with the general bedding-plane orientation. Few grains are at a high angle to bedding and these are generally non-perpendicular to bedding. This starting fabric, for specimens prepared in the same way, has been described in detail by Williams et al. (1977).

Shortening of the specimens parallel to bedding generally resulted in kinking of the initial mica fabric and progressive development, by transposition, of a new foliation inclined to the bedding and statistically parallel to the axial-planes of the folds. At low strains, the orientation distribution of the long dimension of mica grains is bimodal and the pattern can commonly be seen to be due to kinking. In the hinge of a fold (e.g. Fig. 3(b)) the bimodal distribution tends to be

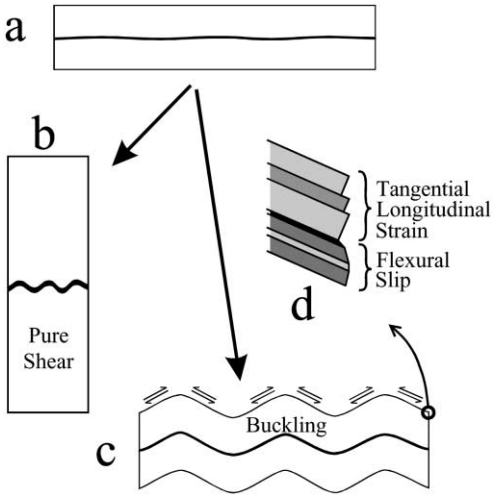

Fig. 4. End-member models of folding. (a) Starting layered sequence with initial deflections in the black layer. (b) Amplification of initial deflections by homogeneous pure shear. (c) Folding by buckling. (d) Two ways in which buckling can be accommodated; tangential longitudinal strain with slip between layers and flexural flow or slip.

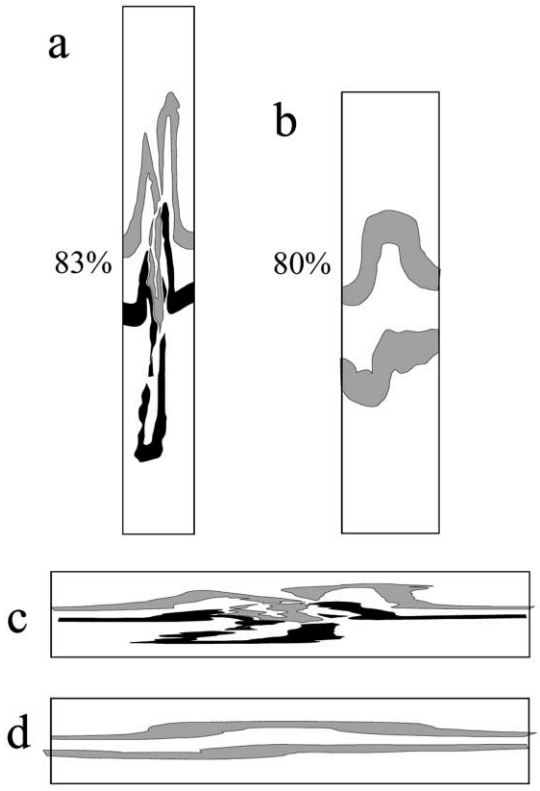

Fig. 5. Specimens 253 (a and c) and 248 (b and d) are shown in their deformed state in (a) and (b) and are restored graphically to their original external shapes in (c) and (d) by homogeneous pure shears orthogonal with the specimen outlines. Restoration was done using CORELDRAW™. It can be seen that the pure shear restores the layering in specimen 248 to something approaching its initial planar configuration. There is no such restoration of specimen 253 indicating that buckling was more significant in the development of folds in this specimen than in specimen 248. Shaded areas represent salt layers; two shades are used in (b) to facilitate separation of layers. See text for discussion.

symmetrical about the axial-plane, whereas on the fold limbs it tends to be asymmetrical with the stronger maximum indicating the same dip as the fold limb, but steeper. The weaker maximum, reflects a dip in the opposite direction to the fold limb. In other words, the distribution is that of asymmetrical parasitic kinks on the fold limb, and such kinks can be recognised in some specimens. As strain increases (as indicated by the marker-grid), the angle between the maxima of the bimodal distribution patterns decreases and a single maximum is approached (cf. Hobbs et al., 1976, p. 248). The experimental conditions are not conducive to recrystallisation, but as pointed out in Williams et al. (1977) and Hobbs et al. (1982), based on experiments where recrystallisation was possible, such mica fabrics are expected to recrystallise to natural-looking foliations.

All these microstructural observations are the same as reported previously in more detail (Williams et al., 1977; Hobbs et al., 1982). One of the high-strain experiments, however, is significantly different. Specimens 248 and 253 (Fig. 1(f) and (g)) were taken to higher strains than any previous experiments, 80 and 83% shortening, respectively. Specimen 248 has a strong axial-plane foliation defined generally by a single preferred orientation of mica (Fig. 3(a)) on fold limbs and in tight fold hinges, and by a symmetrical bimodal fabric in the more open fold hinges (Fig. 3(b)). This is consistent with the previously reported (Williams et al., 1977; Hobbs et al., 1982) general observation that the bimodal fabric contracts to a single maximum with increasing strain. Specimen 253, however, despite the fact that it is the highest-strain specimen does not have an axial-plane foliation. On the fold limbs, the mica fabric and layering are parallel (Fig. 3(c)) and both are parallel to the axial-plane of the folds. It could be argued that transposition of the initial mica fabric is so complete that the observed fabric is an axial-plane foliation. This fabric is indistinguishable from the strongest of the starting fabrics, however, and shows no signs of kinking and transposition into the axial-plane orientation. It is the initial fabric rotated en masse with the fold limb, and further flattened during the late stages of folding. In the fold hinges, the fabric can be traced around the closures (Fig. 3(d)). Locally, as on the left side of the hinge in Fig. 3(d), the relationship is obscured by late shear-bands, but there is no evidence of an axial-plane fabric. In the less-angular hinges, there are occasional parasitic micro-kinks. These kinks are quite open compared with the larger isoclinal folds and compared with the micro-kinks in Fig. 3(b). They represent the earliest stages of axial-plane foliation development, but contrary to the normal situation, they are believed to have developed late, in response to the late pure shear (PS) flattening of the folds (it is significant that these kinks are only found in the hinges where the bedding-parallel foliation remains parallel to the shortening direction throughout the strain history).

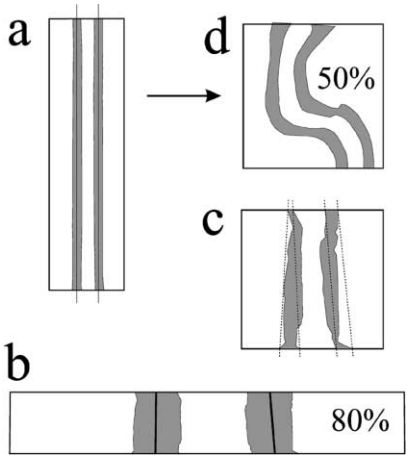

Fig. 6. (a) A tracing of a specimen as it appeared when removed from the rig, after being subjected to confining pressure only. The figure was prepared by first scanning a photograph (× 4 enlargement) of the specimen, then digitally tracing the grid points and the outline of the specimen and salt layers from the image. There is a potential error in identifying the centre of each grid point, but the error is small compared with the misalignment of the points. The curvature of the bedding surfaces is readily seen both in the original photograph and in this figure by placing the photograph or page at an acute angle to the line of sight so that the lines are foreshortened. Straight vertical lines are drawn through the top centre point of the two salt layers. The line through the left-hand layer passes almost through the bottom centre point of the layer, but the line through the right-hand salt layer is clearly left of bottom centre, indicating the slope of that layer. (b) A foreshortened image of the same specimen, prepared digitally by applying an 80% pure shear shortening, using CORELDRAW™. The initial image (see (a) above) used in this procedure was an order larger than the real specimen so that there is no significant error involved in the procedure. The heavy lines, within the salt layers, join the centre points of the ends of each layer. (c) To further accentuate the initial perturbations the salt layers were "thinned" by simply moving the bounding lines closer together, maintaining their original shape. The resulting image was then enlarged. The dashed lines join the outside end points of each salt layer. (d) The actual specimen after 50% shortening. See text for discussion.

4. Interpretation of data

The overall shortening of specimens 248 and 253 is very similar, but the mica fabrics, as well as the folds, are quite different. There is a lack of thickening, commensurate with the overall shortening, in some of the fold hinges and general extension of the limbs in the salt layers of specimen 253. This is consistent with the bulk shortening of the specimen being achieved by bending in the hinges and rotation of the limbs. It indicates that the specimen underwent buckling at an early stage in its history. Specimen 248 on the other hand shows considerable thickening of the salt layers both in the fold hinges and on the limbs, indicating that there was considerable shortening of these layers either prior to, or early in, the buckling process. We can think of this in terms of two end-member types of behaviour. A specimen can shorten by a homogeneous shortening (used in its strict geometrical sense) parallel to layering, in other words a homogeneous PS, or it can shorten by buckling with no change in the thickness of the layers. The homogeneous shortening can only produce folds by passive amplification of pre-existing perturbations (Fig. 4(b)), but the end-members can be combined to produce folds with variable appearance in profile (e.g. Ramsay, 1962, 1967, p. 411; Hudleston, 1973; Treagus, 1982).

The kinematic description of a homogeneous shortening is a pure shear. If there is competence contrast there is a departure from strict homogeneous behaviour. At the lower limb dip, the kinematic description still approaches pure shear in all layers, but as limb dip increases, the bulk shortening is partitioned into individual layers and the kinematics are no longer homogeneous pure shear (cf. "partitioned flattening" of Treagus, 1997). Buckling is a mechanical term that is associated with more than one kinematic description. Two end-member descriptions of buckling are flexural slip or flow (Turner and Weiss, 1963, p. 473; Ramsay, 1967, p. 391) and tangential longitudinal strain (Ramsay, 1967, p. 397). The latter has to be accommodated in a multilayer sequence, by discrete slip between layers or by flexural flow in intervening incompetent layers. We are not concerned, in this paper, with these details of the kinematics which will depend on details of the rheology of the component layers, but note that in all our experiments there is some bedding-parallel shear in all the beds, although it may be small, especially in the salt layers.

We believe that the folds in specimen 248 involved a little buckling and a large PS component during folding, whereas specimen 253 involved strong buckling, and at most, a small PS component, which may have been largely post folding. This difference is demonstrated graphically in a qualitative way in Fig. 5, where homogeneous PS's have been applied to the deformed specimens to restore their original external shape. For specimen 248 this is largely sufficient to restore the initial shape of the layers in that the remaining deflections are quite small. On the contrary, for specimen 253, the layers are still strongly folded, indicating the more significant role of buckling. Other specimens illustrated in Fig. 1 are interpreted as involving a little buckling and a large PS component. In all of them the PS component seems more significant than in specimen 253, but by comparing specimens that have been subjected to similar strains it can be seen that the relative roles of PS and buckling vary from specimen to specimen.

The question has to be asked, therefore, why buckling started at different stages in different experiments, and in particular why there is such a difference between specimens 248 and 253? Intuitively, initial perturbations seem a possible explanation. In classic folding theory (e.g. Biot, 1957; Ramberg, 1963; Chapple, 1969; Fletcher, 1974, 1977; Smith, 1977, 1979), infinitesimal random perturbations trigger buckling but subsequent growth of folds obeys the Biot–Ramberg dominant wavelength relationship and is independent of the perturbations. This independence has been demonstrated by numerical experiments (Zhang et al., 1996) for Maxwell and Mohr–Coulomb materials. The wavelength is believed to be related to the relative thickness

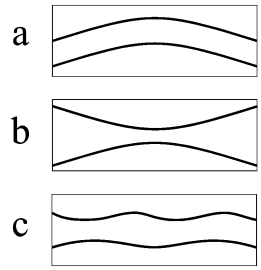

Fig. 7. Cartoon representation of perturbations. Thick black lines represent strong elements in a weak matrix. (a) Perturbations reinforce one another so the system is weak. (b) Perturbations exactly balance one another making the system strong. (c) General situation with random perturbations. See text for discussion.

and rheology of competent and incompetent layers. Large perturbations (deflections of the order of 10°), however, were shown to largely control fold morphology in experiments by Bailey Willis at the turn of the century (these experiments are described and discussed extensively by Johnson (1970)). More recent experiments are described and analysed by Abbassi and Mancktelow (1990) and Mancktelow (1999). Mancktelow (1999) reported results of numerical experiments performed under conditions identical to those of Zhang et al. (1996) in all respects except for a lower strain-rate (see also Zhang et al., 1999). He showed that the fold development was not Biot–Ramberg wavelength growth as reported by Zhang et al. (1996). Instead, the fold geometry is controlled by initial perturbations. Zhang et al. (1999) have subsequently shown that the difference in behaviour is due to variation in strain-rate. At a strain-rate of 10^{-6}, behaviour is dominantly elastic, and the Biot–Ramberg wavelength develops. At a strain-rate of 10^{-12}, behaviour is dominantly viscous, and amplification of initial perturbations dominates. The relative significance of elastic and viscous behaviour, at a given strain-rate, is measured by the Deborah number (Zhang et al., 1999). The folds produced in our experiments are obviously not Biot–Ramberg dominant wavelength folds because they are far from reproducible despite very little difference in the initial specimens in terms of layer thicknesses and the nature of the materials.

The experiments described here differ from those of Bailey Willis, Abbassi and Mancktelow and Mancktelow in that deflections of bedding are much less obvious, but because the starting material is crystalline and simulates natural fabric anisotropy, there are also potential perturbations in the form of random variation in composition and in the preferred orientation of the mica grains. In addition, although small, deflections of bedding are present; this can be demonstrated by scanning large photographic images and digitally tracing the salt-layer contacts. In specimens photographed before deformation, after being subjected to confining pressure, a lack of planarity is recognisable (Fig. 6(a)).

An argument can be made for a correlation between initial deflections and final geometry. This is demonstrated in Fig. 6, where the comparison is made between initial deflections in a specimen and the folds present after 50% shortening. There is not a one-to-one correlation between the initial perturbations in the salt layer contacts and the final folds. There is, however, an initial asymmetry that is reflected in the asymmetrical folds (cf. Abbassi and Mancktelow, 1990). Examination of Fig. 6 shows that the left-hand salt layer is almost parallel to the axis of the specimen and therefore almost parallel to the shortening direction; although difficult to detect in Fig. 6(a), a slight clockwise asymmetry is visible in the foreshortened image (Fig. 6(b)). The right-hand layer, however, is more asymmetrical in an anticlockwise sense (see Fig. 6(b)). This difference in asymmetry is further demonstrated in Fig. 6(c) and is reflected in the asymmetry of the folds (Fig. 6d). In Fig. 6(c), curvature of the left-hand layer suggests a fold closing to the right, whereas the right-hand layer suggests a fold closing to the left. Of the two, the right-hand layer is the more strongly curved (Fig. 6(c)), and might therefore be expected to dominate the folding as is observed in Fig. 6(d). The perturbations in shape are subtle, but they are consistent with the final structure and it seems likely that they have influenced its development.

We were unable to actually examine the role of fabric heterogeneity because we were unable to continue an experiment after a detailed examination of the initial specimen. We know, however, that the initial fabric within any given layer generally varies from point to point, as does the relative abundance of salt and mica. The principal fabric difference is in the degree of preferred orientation of the mica (cf. Williams et al., 1977), and we suggest that this difference and/or difference in composition are likely to be reflected in a variation in strength within a layer (cf. Cobbold et al., 1971; Cobbold, 1976). For example, consider two volumes of a given layer. In one volume, the micas have a preferred orientation such that a fold-like deflection is defined with its axial-plane perpendicular to the layering. A second volume has a bow-tie distribution with all mica grains approximately parallel to the bedding plane, with low angle symmetrical variance about that orientation. If both specimens are subjected to layer-parallel shortening, the volume with the pre-existing deflection is likely to be weakest because it has a built-in buckling weakness. If both volumes exist in the same layer, then everything else being equal, the layer might be expected to bulge where the initial fabric weakness existed. We observe such bulges where no other obvious explanation exists and we believe that these bulges, however they form, can initiate buckling by applying a bending moment to adjacent competent layers which when bent become prone to buckling. By analogy, a bent column will support less load than a straight one, other things being equal.

In a material like that used for this experiment, there are numerous perturbations that appear to affect the folding process. We can represent the perturbations (due to whatever

cause—initial deflection, or variation in initial fabric or composition), that may trigger buckling, diagrammatically by curved lines as in Fig. 7, where the background material is considered mechanically isotropic. If two perturbations reinforce one another (have the same sign) as is shown in Fig. 7(a), the system can be expected to fail by buckling and will experience weakening until the folds become tight and begin to lock-up. If two perturbations are equal and opposite in sign (Fig. 7(b)), buckling is not likely to occur because the two elements stabilise one another and the symmetry of the system will result in a PS shortening parallel to the symmetry plane. In real materials, as deformation proceeds, asymmetry is likely to develop by amplification of small perturbations, and buckling is then likely to occur. We would expect, however, that multilayer systems in general would have randomly distributed perturbations, which can be represented by irregular, out-of-phase curves (Fig. 7(c)). Such a system is less likely to weaken than that shown in Fig. 7(a) and would tend to combine buckling and, as perturbations at various scales competed with one another, to control the position and sign of folds. As deformation proceeds, we would expect the system to become progressively organised and dominated at various scales by folds that would be perpetuated throughout the remainder of the folding process.

Applying the argument to our experiments, we believe that initial deflections and variation in strength due to heterogeneity of fabric or composition were mutually reinforcing in specimen 253 so that buckling occurred early, perhaps at the very start of the experiment. There was little resistance to this and, as a result, buckling dominated the process, and the PS component was relatively insignificant until folding ceased to be a viable shortening mechanism. At that stage, the PS component probably became significant, as indicated by the boudinage of the fold limbs and thickening of the hinges. In other specimens perturbations initiated buckling, but because of perturbations of opposite sign, the buckling was inhibited in the sense that it did not dominate the process, and the PS component continued to play a role in shortening throughout folding. Since the initial perturbations were not reproducible the folds also were not reproducible.

It is significant that the folds in specimen 253 are cylindrical, whereas the folds in specimen 248 are not (Fig. 2). The sort of perturbations considered here are not likely to be geometrically linear in general and, when linear, are not likely to be oriented perpendicular to the direction of shortening. In the case of end-member buckling (no PS component), once initiated, a buckle might be expected to propagate in a direction at a high angle to shortening, because an incipient buckle results in a bending moment being applied to adjacent parts of the layer. Continuing deformation would rotate it progressively closer to an orientation perpendicular to the shortening direction. In the case of buckling with a large component of PS there would be conflicting perturbations and less of a tendency for any one of them to propagate far. Thus the folds might be expected to be non-cylindrical.

5. Foliation development

In our experiments axial-plane foliation development is initiated early in the shortening process leading to folding, as is commonly the case in rocks (e.g. Knipe and White, 1977; Nickelsen, 1979; Williams, 1979; Henderson et al., 1986; Kraus and Williams, 1998). Much shortening occurs during folding, however. If the micro-kinks are not initiated early in the folding process they are less likely to initiate on the fold limbs once significant dip has developed. This is simply because layer-parallel shortening as a function of bulk strain decreases rapidly as limb dip increases. We observe well-developed penetrative kinks at a high angle to bedding in all specimens, including the least deformed (shortened approximately 20%), except specimen 253, which lacks an axial-plane foliation or any kinks on the fold limbs. Taken together, these observations support the argument that penetrative micro-scale buckling is initiated before large-scale buckling becomes the significant shortening mechanism.

Localised micro-scale buckling can occur at any stage in areas where there continues to be foliation-parallel shortening after initiation of the large buckles. For example the open micro-kinks in the fold hinges of specimen 253 occur in a position where the bedding-parallel foliation remained parallel to the bulk shortening direction throughout the experiment. The foliation would therefore have been subjected to a PS component which would have increased during the late stages of the experiment; hence the kinks and the thickening of the hinge. Had the strain been large enough, an axial-plane foliation would have developed in the fold hinge, but not on the limbs. The restriction of these kinks to the fold hinge further supports the argument that kinks have to develop early on the fold limbs, before a critical dip is reached, or they will not develop at all.

6. Discussion

Modelling of folding in multilayer systems is commonly concerned with what might be termed perfect systems in that the material is generally considered homogeneous and the layers parallel and planar. The necessity of perturbations to cause a buckling instability is implicit, but the final geometry is related to layer thickness and relative rheologies, and is independent of the perturbations. In this paper we are concerned with the role of imperfections in such multilayer systems. In perfect systems, the relative roles of buckling and PS are believed to be a function of competency contrast between the various layers. For example, Treagus (1997) demonstrates that if the competency contrast (expressed as viscosity ratio) is as high as 50, some form of buckling will be initiated without a significant

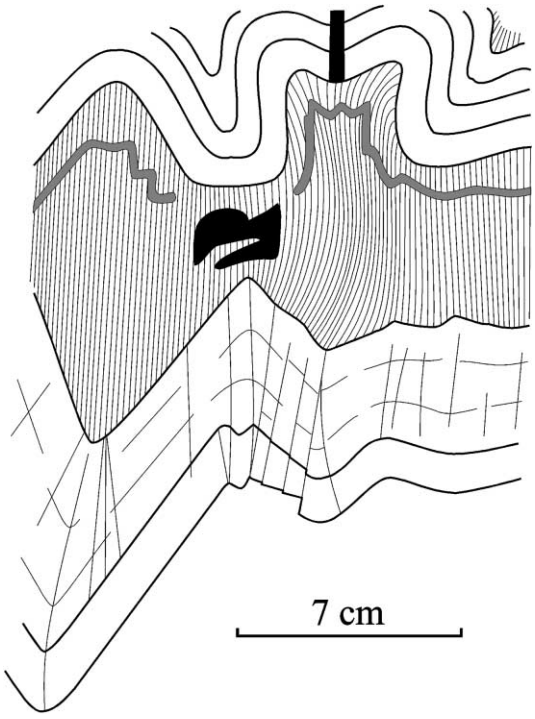

Fig. 8. F2 folds in turbidites, Bermagui, Australia. Closely spaced lines represent the axial plane cleavage in a pelitic layer. Note how the cleavage joins antiforms to synforms in adjacent sandstones. Black areas represent vein quartz.

PS component until the folds become too tight to efficiently accommodate the shortening.

Following this argument, the competency contrast in specimen 253 should be close to 50. We consider this unlikely. We have no directly applicable data, but other experiments suggest that a contrast of approximately two is much more likely. (1) Non-layered specimens of the salt and salt–mica mix, prepared in the same way as the specimens described here, and shortened perpendicular to the foliation under similar conditions (Means and Williams, 1972) have flow-strengths (differential-stress) that differ, in a complex way, by a factor of no more than two. The flow-strength of the salt is fairly constant, but the flow-strength of the salt–mica schist specimens varies with strain. At low strains ($<$15%) they are generally stronger than the salt specimens by as much as 40%; at strains of 10–20% they weaken rapidly and the strength drops to approximately half that of the salt. The drop in strength coincides with the development of conjugate shear-bands and this is interpreted as an indication that the weakening is due to the development of a new deformation mechanism in the form of the shear-bands. Prior to development of the shear-bands, the deformation is unable to exploit the initial anisotropy. After the initiation of the shear-bands, initial and imposed anisotropy play a role in deformation. Similar behaviour might be expected in specimens shortened parallel to the foliation with weakening of the salt–mica schist as kinks develop (cf. Williams and Price, 1990). (2) In experiments on a KCl–mica schist, the flow-strength of the schist peaks at values between approximately 15 and 55 MPa (Williams and Price, 1990) depending on the orientation of the foliation with respect to the shortening direction. Whereas the flow-strength of a pure KCl specimen under the same conditions shows work hardening, and peaks at a little over 20 MPa, at an angular shear of 30° (unpublished data—specimen 237 in Williams and Price, 1990). The weakest specimen is a schist with the foliation in an orientation that favours kinking.

The large PS component present in most of our experiments is consistent with a low competency contrast (cf. Treagus, 1997; Abbassi and Mancktelow, 1990). In terms of the properties of perfect systems, however, we cannot explain specimen 253 because there is no reason why it should have a significantly different competency contrast to specimen 248. We therefore need some other factor to explain the significant difference between specimens 248 and 253 and we believe that the factor is the initial imperfections in the system.

It could be argued that all specimens behaved as reasonably perfect systems, except for specimen 253 which was the only one affected by initial perturbations. If this were correct, however, better reproducibility should have been achieved in all but specimen 253. Perhaps a better explanation of the similarity in these results, that is capable at the same time of explaining the differences, is that perturbations played a role in all of the experiments. Most specimens were sufficiently symmetrical, however, in terms of the distribution, sign and strength of the perturbations, to hinder buckling and encourage PS. The resulting structures are similar because PS was a large component in each experiment, but they differ because its relative magnitude varied from one experiment to another.

The foliation may be the main factor in this process. The strength of such an anisotropic material is dependent on the orientation of the plane of anisotropy to the stress axes (cf. Cobbold, 1976). A deflection in the orientation of a bedding plane is likely to result in a similar deflection in the orientation of the statistically defined foliation plane, because during pressurisation of the specimen, compaction must be achieved by bending of the wafers to accommodate initial variations in thickness. Such built-in deflections will amplify (cf. Cobbold et al., 1971; Cobbold, 1976) if not balanced by other similar deflections of opposite sign or some other feature, such as a strong layer capable of withstanding the bending moment, being applied to it by the adjacent buckling layer.

Fold-modelling of competent layers sandwiched between incompetent layers is capable of explaining the periodicity of folds (e.g. Johnson, 1970) and this might be seen as an argument against the model presented here. The two models are not incompatible, however. A sufficient degree of perfection may exist in some natural multilayer systems for the dominant wavelength type model to be appropriate. We do not know how to quantify the significance of perturbations. If they were purely geometrical, the problem might

be fairly simple. However, since ultimately they are due to variation in mechanical properties, all factors such as fluid content, strain-rate, temperature and gradients in all of these factors, become additional ingredients; quantification then becomes difficult, if not impossible. However, we presume that there will be perturbations that are too "small" (whatever their origin) relative to other factors, to influence fold morphology, although they may trigger an instability. The dominant wavelength-type model might also be appropriate in rocks where there is a much greater competency contrast such that perturbations become comparatively insignificant. Alternatively, the same model may be appropriate in situations where perturbations exist but are statistically symmetrical. In less perfect systems, including statistically asymmetrical systems, the model proposed here may be more appropriate. In addition, we suggest that the distribution and nature of a large number of perturbations may in itself result in a degree of periodicity in folds. It might be expected that such periodicity would be imperfect, but then the periodicity of fold trains is commonly less periodic than might be expected if wavelength was simply a function of thickness and relative rheology. Finally, it is possible that both mechanisms operate synchronously as competing processes.

As evidence that perturbations may be relevant to folding in rocks, we cite the existence of folds such as the example in Fig. 8. The folds in two adjacent sandstone layers share a common axial-plane with a cleavage passing from one hinge to the other, but one fold is synformal and the other is antiformal. For the two folds to bend in opposite directions requires a large volume of material in the intervening incompetent layers to migrate into the space created by the folds. We suggest that the only way of developing this structure is by the existence of significant perturbations in the original layered sequence.

In our experiments, axial-plane cleavage is generally initiated before larger-scale folding. The bimodal mica fabrics which develop initially, have their counterpart in nature, where the role of kinking in the development of foliation can commonly be demonstrated (Williams et al., 1977). Evidence for axial-plane foliations being initiated prior to folding is common in rocks (Knipe and White, 1977; Nickelsen, 1979; Williams, 1979; Henderson et al., 1986; Kraus and Williams, 1998) and explains why cleavage is refracted as it passes through layers of different competence. There remains, however, the possibility that some locally (i.e. local on the scale of individual folds) developed axial-plane foliations may develop late during folding.

The cleavage is itself a product of folding and as such may also be due to pre-existing perturbations. There must obviously be a relationship between the scale of perturbations and the scale of related folds. Grain-scale variation in the orientation of mica grains may be the cause of the microfolding that gives rise to the cleavage. The bow-tie distribution lends itself to such a process. The reason that microfolds (cleavage) are commonly initiated before the large folds may be due to the fact that there is commonly a greater variation in the orientation of mica grains than there is in the orientation of layering (i.e. the small-scale variation is greater than the large-scale variation). In addition, this mechanism explains the marked correlation (e.g. Williams, 1990) between grain size and spacing of septa in crenulation cleavage.

Ultimately, the problem seems to be one of the manner in which the rock shortens. If buckling is the dominant process, a Biot–Ramberg dominant wavelength is likely. If PS is dominant then amplification of pre-existing deflections and deflections developed by weak buckling during the deformation, is likely to control wavelength. There may be many factors important in deciding which process is dominant. Zhang et al. (1999) have shown that, for elastic viscous materials, the dominant process can be decided by the Deborah number. Other factors may include competency contrast and, as suggested by the data presented here, distribution and scale of heterogeneity of anisotropy. A possibility that needs to be explored further is that perturbations become important when competency contrast is small. This is particularly important if we are correct in interpreting axial-plane foliations as evidence of low competency contrast, since the common occurrence of axial-plane foliations would then suggest that competence contrast is commonly low in natural situations.

7. Conclusions

1. Perturbations probably play a significant role in the development of the shape and distribution of natural folds. We do not see the perturbation model as an alternative to fold-models based on perfect multilayer sequences, but see it as reflecting an additional factor that is likely to vary in importance in different natural situations. Perturbations may be the dominant factor in the development of some folds (e.g. Fig. 8); in other situations they may have little significance. The type of perturbation that we consider significant would be anything that can cause a variation in the load-bearing capacity of a layer; for example, pre-existing deflections in the layer or one of its contacts, and local variation in microfabric and/or composition within a layer (in other words, anything that might cause local variation in mechanical properties).
2. Geometrical perturbations are probably comparatively simple. Perturbations due to variation in mechanical properties are likely to be complex and will be influenced by environmental factors such as fluid pressure, strain-rate and temperature, and gradients in these factors. It may be impossible to quantify their effect, except by empirical means, for individual specimens.
3. Depending on the symmetry, or lack thereof, of the perturbations, either end-member buckling or PS may

be the dominant process involved in layer-parallel shortening, or any combination of the two.

4. The presence of a penetrative foliation on the limbs of a fold as well as in the hinge indicates that folding has involved a significant PS component (at the scale of the fold)—either pre-folding or early during folding. If the buckling component has been weak, such a cleavage may show little refraction.
5. The lack of an axial-plane cleavage on the limbs of a fold indicates that buckling has been more important than the PS component at least in the early stages of folding. The presence of an axial-plane cleavage in the hinge of such folds combined with boudinage of layering on the limbs, is an indication that the PS component became significant during the late stages of folding.
6. The stronger the buckling component relative to the PS component, the more cylindrical the folds are likely to be. The converse is also true.
7. The scale of folding can be related to the scale of the initial perturbations.

Acknowledgements

We gratefully acknowledge Win Means for discussion, training in experimental procedures and for the use of his deformational laboratory. The paper benefited from criticism from Sue Treagus and from formal reviews by Simon Hanmer and Wouter Bleeker. The experiments were performed in 1974 and PFW acknowledges the travel assistance from the State University of Leiden. PFW also acknowledges a Research Grant from NSERC. Drafting assistance from Angel Gomez is also gratefully acknowledged.

References

Abbassi, M.R., Mancktelow, N.S., 1990. The effect of initial perturbation shape and symmetry on fold development. Journal of Structural Geology 12, 273–282.

Biot, M.A., 1957. Folding instability of a layered viscoelastic medium under compression. Poceedings of the Royal Society of London, Series A 242, 444–454.

Biot, M.A., 1961. Theory of folding of stratified viscoelastic media and its implications in tectonics and orogenesis. Bulletin of the Geological Society of America 72, 1595–1620.

Biot, M.A., Odé, H., Roever, W.L., 1961. Experimental verification of the theory of folding of stratified viscoelastic media. Bulletin of the Geological Society of America 72, 1621–1630.

Chapple, W.M., 1969. Fold shape and rheology. The folding of an isolated viscous–plastic layer. Tectonophysics 7, 97–116.

Cobbold, P.R., 1976. Mechanical effects of anisotropy during large finite deformations. Bulletin de la Société géologique de France 7, 1497–1510.

Cobbold, P.R., 1983. Kinematic and mechanical discontinuity at a coherent interface. Journal of Structural Geology 5, 341–349.

Cobbold, P.R., Cosgrove, J.W., Summers, J.M., 1971. Development of internal structures in deformed anisotropic rocks. Tectonophysics 12, 23–53.

Fletcher, R.C., 1974. Wavelength selection in the folding of a single layer with power-law rheology. American Journal of Science 274, 1029–1043.

Fletcher, R.C., 1977. Folding of a single viscous layer, exact infinitesimal-amplitude solution. Tectonophysics 39, 593–606.

Ghosh, S.K., 1993. Structural Geology. Fundamentals and Modern Developments.. Pergamon Press, Oxford.

Henderson, J.R., Wright, T.O., Henderson, M.N., 1986. A history of cleavage and folding: an example from the Goldenville Formation, Nova Scotia. Geological Society of America Bulletin 97, 1354–1366.

Hobbs, B.E., Means, W.D., Williams, P.F., 1976. An Outline of Structural Geology. John Wiley, New York.

Hobbs, B.E., Means, W.D., Williams, P.F., 1982. The relationship between foliation and strain: an experimental investigation. Journal of Structural Geology 4, 411–428.

Hudleston, P.J., 1973. An analysis and interpretation of minor folds developed experimentally in viscous media. Tectonophysics 16, 189–214.

Hudleston, P.J., Lan, L., 1994. Rheological controls on the shapes of single-layer folds. Journal of Structural Geology 16, 1007–1021.

Hudleston, P.J., Stephansson, O., 1973. Layer shortening and fold-shape development in the buckling of single layers. Tectonophysics 17, 299–321.

Johnson, A.M., 1970. Physical Processes in Geology. W.H. Freeman, San Francisco, CA.

Knipe, R.J., White, S.H., 1977. Microstructural variation of an axial plane cleavage around a fold—a high voltage electron microscope study. Tectonophysics 39, 355–380.

Kraus, J., Williams, P.F., 1998. Relationships between foliation development, porphyroblast growth and large-scale folding in a metaturbidite suite, Snow Lake, Canada. Journal of Structural Geology 20, 6176.

Mancktelow, N.S., 1999. Finite element modelling of single-layer folding in elasto-viscous materials: the effect of initial perturbation geometry. Journal of Structural Geology 21, 161–177.

Means, W.D., 1975. Natural and experimental microstructures in deformed micaceous sandstones. Bulletin of the Geological Society of America 86, 1221–1229.

Means, W.D., Williams, P.F., 1972. Crenulation cleavage and faulting in an artificial salt–mica schist. Journal of Geology 80, 569–591.

Nickelsen, R.P., 1979. Sequence of structural stages of the Alleghany Orogeny, at the Bear Valley Strip Mine, Shamokin, Pennsylvania. American Journal of Science 279, 225–271.

Parrish, D.K., 1973. A nonlinear finite element fold model. American Journal of Science 273, 318–334.

Ramberg, H., 1959. Evolution of ptygmatic folding. Norsk Geologisk Tidsskrift 39, 99–151.

Ramberg, H., 1963. Fluid dynamics of viscous buckling applicable to folding of layered rocks. Bulletin of the American Association of Petroleum Geologists 47, 484–505.

Ramberg, H., 1964. Selective buckling of composite layers with contrasted rheological properties. A theory for simultaneous formation of several orders of folds. Tectonophysics 1, 307–341.

Ramsay, J.G., 1962. The geometry and mechanics of formation of "Similar" type folds. Journal of Geology 70, 309–327.

Ramsay, J.G., 1967. Folding and Fracturing of Rocks. McGraw-Hill, New York.

Ramsay, J.G., Huber, M., 1987. The Techniques of Modern Structural Geology. , Folds and Fractures, Vol. 2. Academic Press, London.

Sherwin, J.A., Chapple, W.M., 1968. Wavelengths of single layer folds: a comparison between theory and observation. American Journal of Science 266, 167–179.

Smith, R.B., 1977. Formation of folds, boudinage, and mullions in non-Newtonian materials. Geological Society of America Bulletin 88, 312–320.

Smith, R.B., 1979. The folding of strongly non-Newtonian layer. America Journal of Science 279, 272–287.

Treagus, S.H., 1981. A theory of stress and strain variations in viscous layers, and its geological implications. Tectonophysics 72, 75–103.

Treagus, S.H., 1982. A new isogon-cleavage classification and its application to natural and model fold studies. Geological Journal 17, 49–64.

Treagus, S.H., 1993. Flow variations in power-law multilayers: implications for competence contrasts in rocks. Journal of Structural Geology 15, 423–434.

Treagus, S.H., 1997. Modelling of deformation partitioning in folds. In: Sengupta, S. (Ed.). Evolution of Geological Structures in Micro- to Macro-scales. Chapman Hall, London, pp. 341–372.

Treagus, S.H., Sokoutis, D., 1992. Laboratory modelling of strain variation across rheological boundaries. Journal of Structural Geology 14, 405–424.

Turner, F.J., Weiss, L.E., 1963. Structural Analysis of Metamorphic Tectonites. McGraw-Hill, New York.

Twiss, R.J., Moores, E.M., 1992. Structural Geology. W.H. Freeman, New York.

Williams, P.F., 1979. The development of asymmetrical folds in a cross-laminated siltstone. Journal of Structural Geology 1, 19–30.

Williams, P.F., 1990. Differentiated layering in metamorphic rocks. Earth Science Reviews 29, 267–281.

Williams, P.F., Price, G.P., 1990. Origin of kinkbands and shear-band cleavage in shear zones: an experimental study. Journal of Structural Geology 12, 145–164.

Williams, P.F., Means, W.D., Hobbs, B.E., 1977. Development of axial-plane slaty cleavage and schistosity in experimental and natural materials. Tectonophysics 42, 139–158.

Zhang, Y., Hobbs, B.E., Ord, A., Mühlhaus, H.B., 1996. Computer simulation of single-layer buckling. Journal of Structural Geology 18, 643–655.

Zhang, Y., Hobbs, B.E., Ord, A., Mühlhaus, H.B. 1999. A clarification of an issue regarding the influence of initial irregularities upon fold shape. Specialist Group in Tectonics and Structural Geology Field Conference, Halls Gap, Australia, February 1999. Geological Society of Australia Abstracts Series, No. 53, p. 278.